

Dynamic necking of notched tensile bars: An experimental study

D. Rittel^{a,b}, Y. Rotbaum^a, J. A. Rodríguez-Martínez^{a,b,*}, D. Sory^{a,c}, R. Zaera^b

^a*Faculty of Mechanical Engineering, Technion. 32000 Haifa, Israel*

^b*Department of Continuum Mechanics and Structural Analysis. University Carlos III of Madrid. Avda. de la Universidad, 30. 28911 Leganés, Madrid, Spain*

^c*Ecole Centrale des Arts et Metiers, Bruxelles, Belgium*

Abstract. The mechanics of necking inception in dynamically-stretched notched specimens have been investigated. For that task, a systematic experimental campaign of quasi-static and dynamic tensile tests on martensitic steel specimens has been conducted. Samples with and without notches have been considered. Unlike the quasi-static tests, the dynamically-tested notched samples revealed that, under certain loading conditions, flow localization may develop away from the groove. The experimental results presented in this investigation show that the presence of sharp geometrical imperfections in ductile materials subjected to dynamic loading does not necessarily dictate the necking and fracture locus.

Keywords: Dynamic necking, Notch, Tensile tests, Weakest link

1. Introduction

Structural elements often exhibit abrupt changes in the cross-sectional area or disruptions of the smooth surface. Grooves, fillets, holes, sharp corners or threads are all examples of geometric discontinuities causing the solid to experience a local increase in the intensity of the stress field which reaches much larger magnitudes than does the average stress over the section, as shown by theoretical analyses and experimental measurements. Notch or stress concentrator (in regard to their geometric features or to their internal force distribution, respectively) is a general term meaning any or all of the above. A theoretical analysis of the role of stress concentrators was firstly highlighted by Inglis (1912) who gave a stress concentration factor for an elliptical defect. Later on, Neuber (1936, 1958) and Peterson (1933, 1953) were concerned with predicting failure in metallic

components, and developed the classical explanations for notch effects. Many analytical equations expressing the distribution of elastic-plastic stress and strain concentration fields at a notch were developed by these two authors. Because of the importance in structural design of notched tension members, the stress-concentration effects on them are of practical interest. The problem has therefore received considerable attention since the pioneering works of Preuss (1912), Cocker, (1912), Cocker et al. (1912) and Howland (1929), up to the more recent due to Strandberg (2001) and Zappalorto and Lazzarin (2011). Notch effects are continuously re-examined by employing experimental, analytical and numerical methods.

A considerable amount of work has been achieved to determine the quasi-static stress concentration factors for common geometrical discontinuities. However, although designers are concerned about high-speed loading applications, relatively few studies have been carried out to examine the behavior of notched bars under dynamic tensile loading. The understanding and documentation of dynamic stress concentration factors has been considered an important field for many areas of mechanical engineering, including crashworthiness, high-speed impact, and transportation of hazardous materials (Altenhof et al., 2004). Experimental (James and North, 1969; Nakayama et al., 1998) and numerical (Matsumoto et al., 1990; Altenhof et al., 2004) techniques have been used to analyze the influence of notch geometry and loading conditions on the differences between quasi-static and dynamic elastic stress concentration factors.

What definitely makes the analysis of notches relevant is that the majority of failures, in both quasi-static and impact conditions emanate from stress concentrators. Therefore, the underlying idea behind all these studies is the consideration of the notch as a structural weak point, hence naturally regarded as a definite source of failure. However, and bearing in mind the undisputed relevance of all the aforementioned analyses for the design of structural elements, it is worth reassessing the problem for dynamic loading conditions. Stated otherwise: Would it be possible to

find a loading condition under which the fracture locus will skip the notch? Based on the experience gained in quasi-static conditions throughout over a century, it seems difficult to respond positively to this question. However, under suitable impact loading, we found a manifest exception to this rule, specifically when wave propagation is strongly present in the loading process. Impact tests designed to characterize the dynamic behavior of materials tend to avoid any phenomenon, usually related to wave propagation, that may hide the real stress-strain characteristic of the material. Some distinctive examples are peaks in the input waves, that may be damped by pulse shapers (Gerlach et al, 2011), or lack of equilibrium, that may be prevented by using short specimens. Alternatively, the propagation of stress waves in the axial direction of the specimen is precluded considering appropriate symmetries in the geometric and loading features of the tests, like in the radial expansion of a ring (Zhang & Ravi-Chandar, 2006, 2008).

In this work, a study has been conducted to assess the effects a stress concentrator may have on a dynamically loaded specimen, in presence of stress waves. For that task, a systematic experimental campaign of quasi-static and dynamic tensile tests of martensitic steel specimens has been conducted. Samples without and with notches, at different locations along the specimen's gauge, were considered. The dynamic experiments revealed that a neck (and subsequent failure surface) may develop away from the notch. The presence of a weak point in the structure will not necessarily dictate the failure locus at high loading rates. Moreover, for identical applied velocities and notch position, the results are quite repeatable and predictable thus strengthening the idea that necking location is deterministic and dictated by dynamic effects, namely stress waves and inertia.

2. Experimental setup

The material of this study is a hardened 15-5 PH steel (condition A), supplied as a 12.7 mm diameter bar, and tested in the as-received condition. This material is a high-strength fully

martensitic steel with additional strengthening due to precipitation. Tensile cylindrical specimens with end threads were machined from the bar. The specimens' dimensions are shown in Fig. 1 and Table 1. Two types of specimens were manufactured: smooth (*no notch*) and notched. The geometry and dimensions of the notches were carefully checked for each specimen after machining using a profilometer, which revealed a natural scatter from one specimen to the other. Only those notches which fulfilled the geometrical requirements listed in Table 2 were considered as valid specimens. The notches were machined alternatively at a distance M, N or L from the loaded end of the sample, as shown in Fig. 1.

Quasi-static and dynamic tests were conducted using both smooth and notched samples, as follows:

- *Quasi-static tests:* The quasi-static tensile specimens were tested using a servo-hydraulic testing machine (MTS 810) under displacement control. A laser optical extensometer (LE-05, EIR) was used for the axial strain measurements. A total of 3 smooth and 3 notched specimens were tested.
- *Dynamic tests:* The dynamic tensile specimens were tested in a 12.7 mm diameter tensile Kolsky apparatus (Split Hopkinson Tensile Bar), made of hardened 17-4 PH-steel, in which the end of the incident bar is loaded by a 320 mm long gas-launched hollow cylindrical impactor. A rotating mirror high speed camera (Cordin 530) was synchronized with the incident bar signals to capture the evolution of the specimen and neck's development during the dynamic tensile tests. The tested impact velocities ranged from 10 to 25 m/s. The applied velocities are determined from the measured incident, reflected and transmitted pulses, as for any other standard test with the Split Hopkinson Tensile Bar. It should be noted that the gauge length is much longer than the diameter of the specimens, which allows for nearly

one-dimensional wave propagation within the sample. Let us remark that wave propagation plays a key role on necking inception as further discuss in forthcoming sections of the paper. A total of 5 smooth and 13 notched specimens were tested.

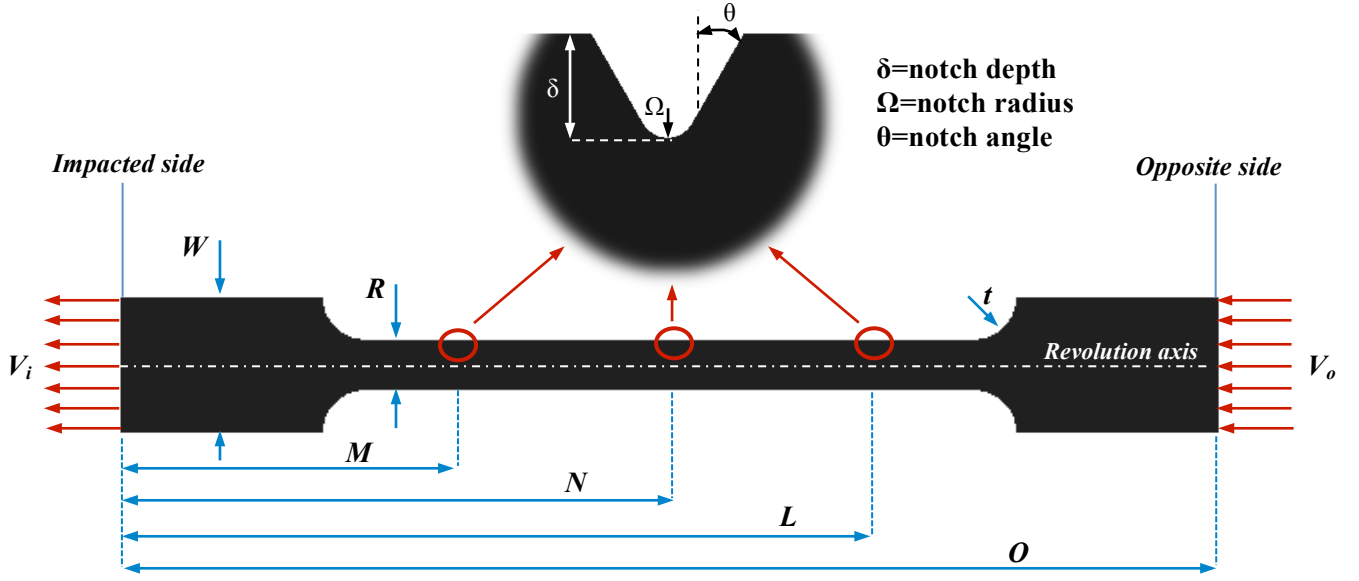


Fig. 1. Geometry of the tensile specimens.

M	N	L	O	R	t	W
26.5	32.5	38.5	65.0	3.0	2.5	8.0

Table 1. Dimensions of the sample (mm).

δ (mm)	Ω (mm)	θ
0.15 ± 0.002	0.05 ± 0.005	$55^\circ \pm 5^\circ$

Table 2. Dimensions of the notch.

3. Quasi-static tests

Typical true stress-strain curves for smooth and notched samples under quasi-static loading are shown in Fig. 2. The 15-5 PH steel possesses a rather high yield strength, $\sigma_y \sim 1100$ MPa, and very limited strain hardening. These are common characteristics shared by many commercial martensitic steels.

It is well known that under quasi-static loading, and therefore an equilibrated specimen, the weakest section dictates the fracture location. Such behavior was indeed observed in the experiments:

- Smooth samples: Fracture was preferentially located close to the middle of the gauge, although it exhibited certain variability. Under ideal conditions the necking location corresponds to the middle of the gauge due to symmetric loading and boundary conditions. However, due to the presence of natural (material) or induced (geometrical) flaws, the weakest section may be occasionally shifted leading to fracture closer to the sample ends, as illustrated in Fig. 2.
- Notched samples: fracture was located in the notch for *all* the tested specimens. The notch was the seed for necking nucleation, accelerating flow localization. The groove reduces the cross-sectional area of the sample and concentrates stresses, therefore acting as the weakest point irrespective of its location in the gauge. Necking inception occurred as soon as the material underwent plasticity. The macroscopic necking strain, here defined as $\varepsilon_n = \varepsilon \big|_{\frac{d\sigma}{d\varepsilon}=0}$, of the notched samples was much smaller, $\varepsilon_n \sim 0.01$, than in the case of the smooth samples, $\varepsilon_n \sim 0.04$, as shown in Fig. 2.

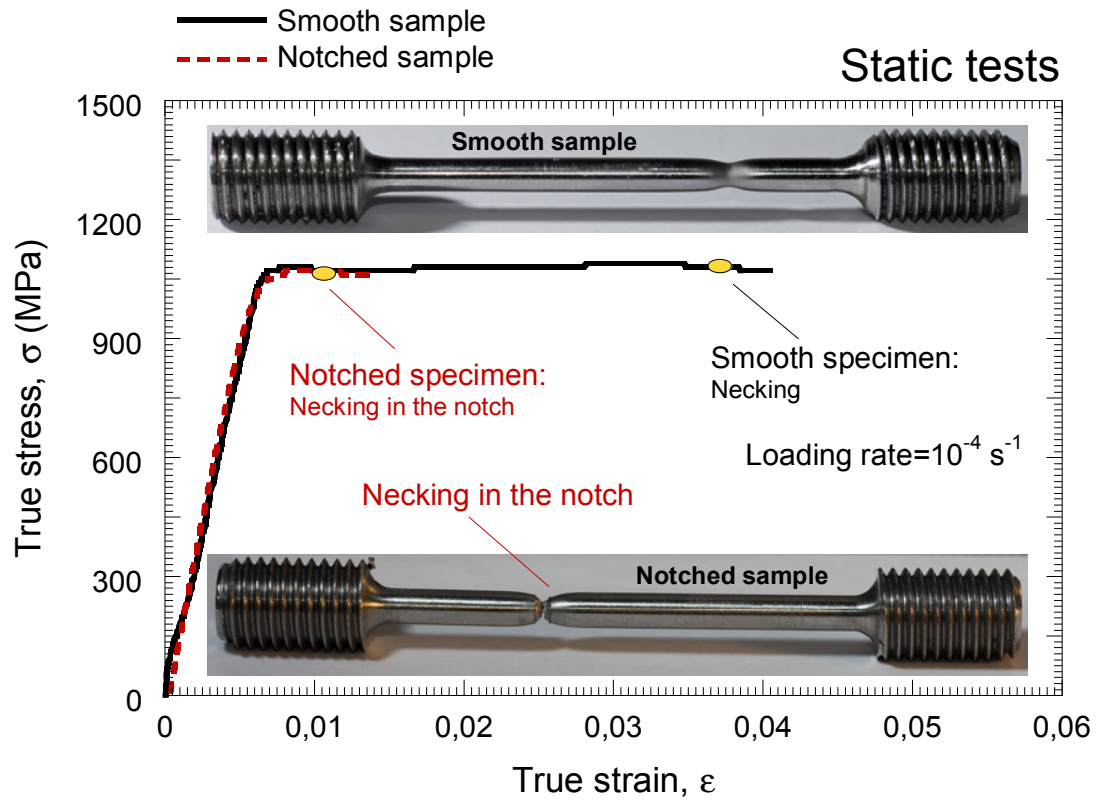


Fig. 2. Typical true stress-strain curves for smooth and notched samples under quasi-static loading. Note the early necking of the notched specimen.

These results, which represent an (another) experimental verification of the weakest link theory in quasi-statics, trigger the following questions:

- Are the quasi-static observations reported here applicable to the dynamic loading case?
- Can one automatically generalize the weakest point approach to cases where stress wave loading and inertia play a dominant role?

4. Dynamic tests

a. Smooth specimens

Table 3 lists the results of the dynamic tensile tests carried out on smooth specimens. As mentioned in Osovski et al. (2013), one should note that the specimen is not rigidly clamped, which results in a small, yet non-negligible, velocity on the transmitted side. Before analyzing the

experimental results, it should be noted that loading velocity is directly related to the stress wave induced in the sample (one may think here about the one dimensional wave propagation theory). Therefore, behind the term “loading velocity” repeatedly invoked in the paper resides the magnitude of the stress wave induced in the specimen by the impact.

Table 3 and Fig. 3 show that when the incident velocity remains equal or smaller than 15 m/s, the neck forms on the impacted side, whereas at higher velocities, it now forms on the opposite side. This trend has been found and thoroughly discussed by the authors in previous works (Rusinek et al, 2005; Rodríguez-Martínez et al, 2013). Note that, in the absence of results for 16 m/s, one can speculate that this velocity is the pivot at which the neck location switches from impacted to opposite side. Altogether, one finds that it is quite difficult to exactly pinpoint the value of this transition velocity, as the transition itself is quite abrupt as a sign of high sensitivity of the neck location to the applied loading (magnitude of the stress wave induced by the impact) and boundary conditions.

Specimen	Input velocity, V_i (m/s)	Output velocity, V_o (m/s)	Neck location
#1	<i>15 (average)</i>	<i>0.85 (average)</i>	<i>Impacted side</i>
#2	<i>13 (average)</i>	<i>0.85 (average)</i>	<i>Impacted side</i>
#3	<i>12 (average)</i>	<i>0.85 (average)</i>	<i>Impacted side</i>
#4	<i>18 (average)</i>	<i>1.00 (average)</i>	<i>Opposite side</i>
#5	<i>17 (average)</i>	<i>1.00 (average)</i>	<i>Opposite side</i>

Table. 3. Summary of the dynamic tensile tests carried out on smooth specimens.

Typical velocity profiles are shown in Fig. 3, for which one can note that they all look relatively similar, without any noticeable feature, other than the magnitude of the input velocity (magnitude of the stress wave induced by the impact), that could cause the observed jump in neck location. One should also note that those results all indicate the high level of reproducibility of the observations as to neck location. These results also reinforce previous conclusions found in Osovski

et al. (2013), Sørensen and Freund (2000) and Rodríguez-Martínez et al. (2013) as to the deterministic character of the neck location in dynamic tensile and ring expansion tests, respectively.

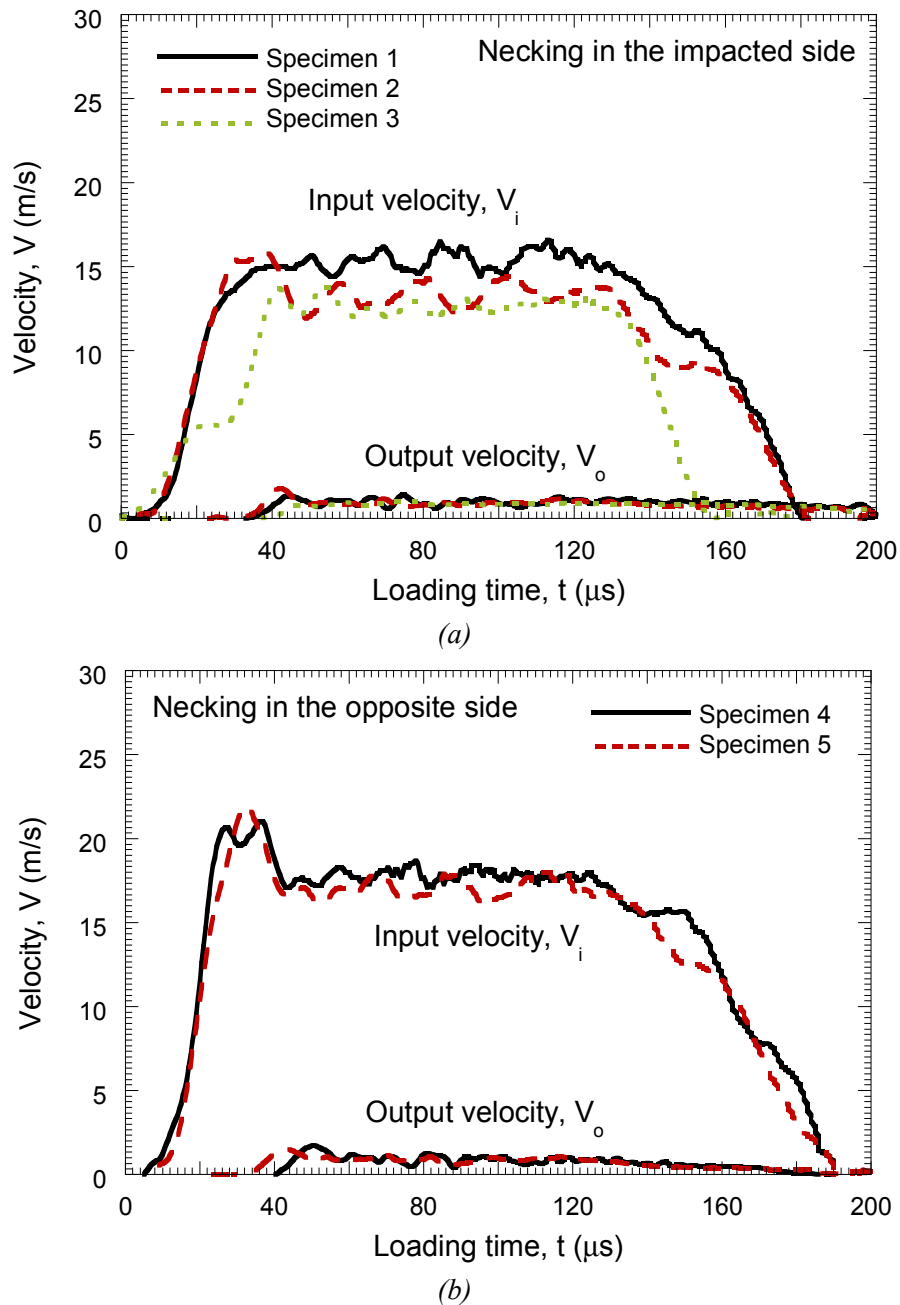


Fig. 3. Input and output velocity profiles of the dynamic tensile tests carried out on smooth specimens. (a) Tests for which the neck is located in the impacted side, (b) tests for which the neck is located in the opposite side.

The corresponding broken specimens are shown in Fig. 3. One noticeable observation is that, irrespective of the location of the neck (impacted or opposite side), the absolute distance of the neck from the fillet is remarkably similar for all the tested specimens.

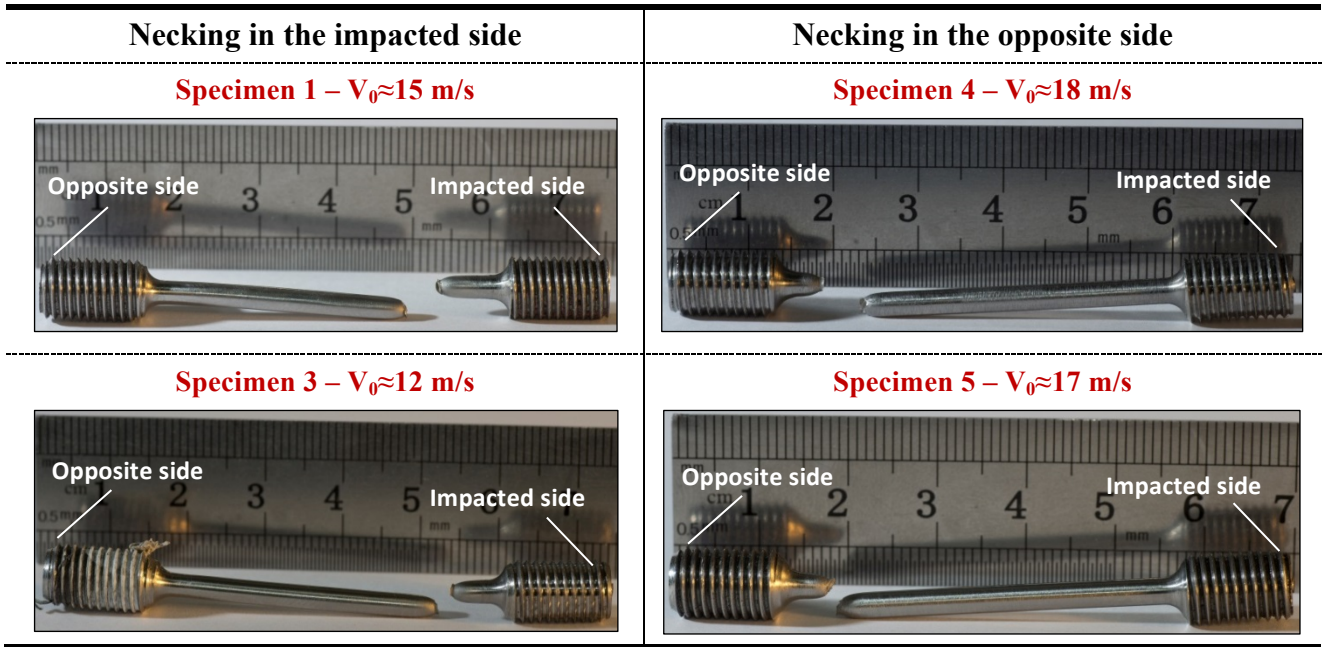


Fig. 4. Tested smooth specimens.

b. Notched specimens

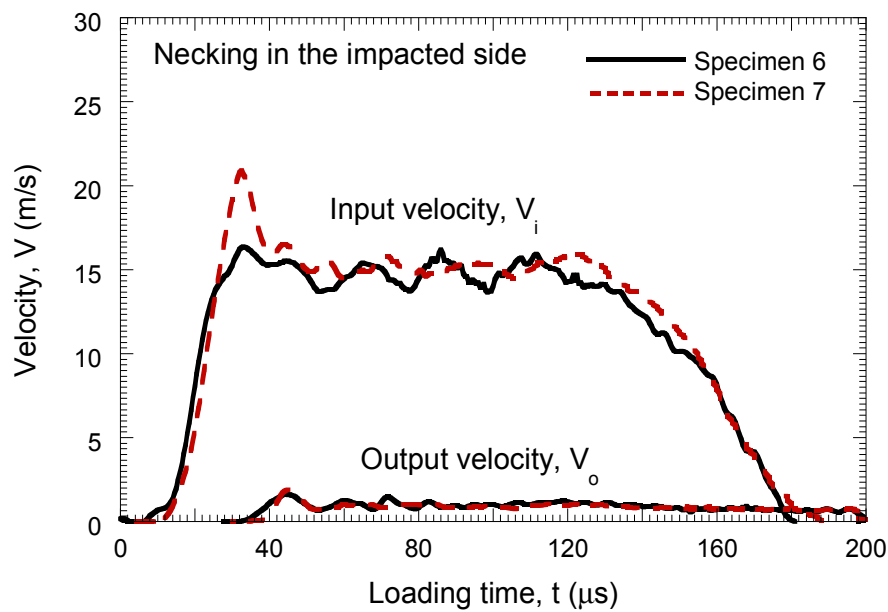
Table 4 lists all the representative dynamic tests that were carried out on centrally notched specimens (notch location N in Fig. 1). The velocity profiles are shown in Fig 5 for each reported experiment. As for the quasi quasi-static case, they all look very similar in shape, except for the higher velocity tests for which an inertial peak is observed, prior to reaching a stable input velocity. Such peak velocities are listed in Table 4. The development of an inertial peak is mostly related to the nature of the test (in which severe accelerations are applied to the system) and the high length to diameter ratio of the samples. As previously mentioned for the dynamic experiments on the smooth samples, the dynamic tests on notched specimens reveal a highly unstable position of the neck that most likely results from a high sensitivity to the loading (magnitude of the stress wave induced by the impact) and boundary conditions applied in the tests. But most of all, the present results clearly show, for the first time to the best of the authors' knowledge, that the presence of a notch (weak or weakest point) does not necessarily dictate the location of the neck, the latter being capable of “ignoring” the notch, Table 4 and Fig. 6. This observation stands at odds with neck location in quasi-static testing.

While the output velocities are all of the same order of magnitude, the results clearly indicate that the neck location jumps from the impacted to the opposite side as the input velocity increases, Fig. 5. Basically, specimens 6-10 develop a neck at the same location than do smooth specimens for similar impact velocities.

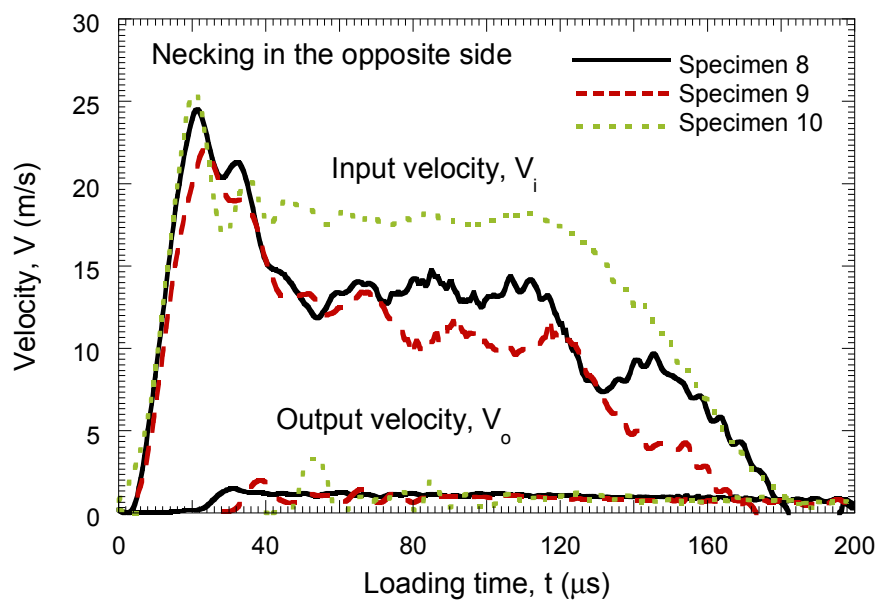
The results also show a “twilight velocity zone” in which the neck is located in the notch (specimens 11-14), and this zone covers both the lower and higher velocities applied in the tests. These specimens do not reveal a specific pattern. However, one interesting observation is shown in Fig. 7. For this specimen (# 14), fracture indeed occurred in the notch but a second diffuse neck was clearly observed on the opposite side, as would be expected for a smooth specimen tested at a similar velocity (within the higher velocities tested). Such observations are quite rare, from an experimental point of view, although they can be predicted by numerical simulations (Rusinek et al. 2005, Rodríguez-Martínez et al. 2009). One can therefore postulate that the “expected” location of the diffuse neck in specimen 14, together with the apparent lack of consistent pattern for specimens 11-14, all suggest some variability in the notch depth as reported in Table 2. While the sensitivity of necking to notch geometry has not been investigated here, it appears to be quite high and this issue certainly deserves additional investigation.

Specimen	Input velocity, V_i (m/s)	Output velocity, V_o (m/s)	Neck location
#6	<i>15.0 (average)</i>	<i>1.1 (average)</i>	<i>Impacted side</i>
#7	<i>15.0 (average)</i>	<i>1.1 (average)</i>	<i>Impacted side</i>
#8	<i>25.0 (peak)</i>	<i>1.3 (average)</i>	<i>Opposite side</i>
#9	<i>21.7 (peak)</i>	<i>0.8 (average)</i>	<i>Opposite side</i>
#10	<i>25.0 (peak)</i>	<i>0.8 (average)</i>	<i>Opposite side</i>
#11	<i>18.8 (peak)</i>	<i>0.9 (average)</i>	<i>Notch</i>
#12	<i>13.3 (average)</i>	<i>0.9 (average)</i>	<i>Notch</i>
#13	<i>16.9 (average)</i>	<i>0.9 (average)</i>	<i>Notch</i>
#14	<i>23.6 (peak)</i>	<i>0.9 (average)</i>	<i>Notch</i>

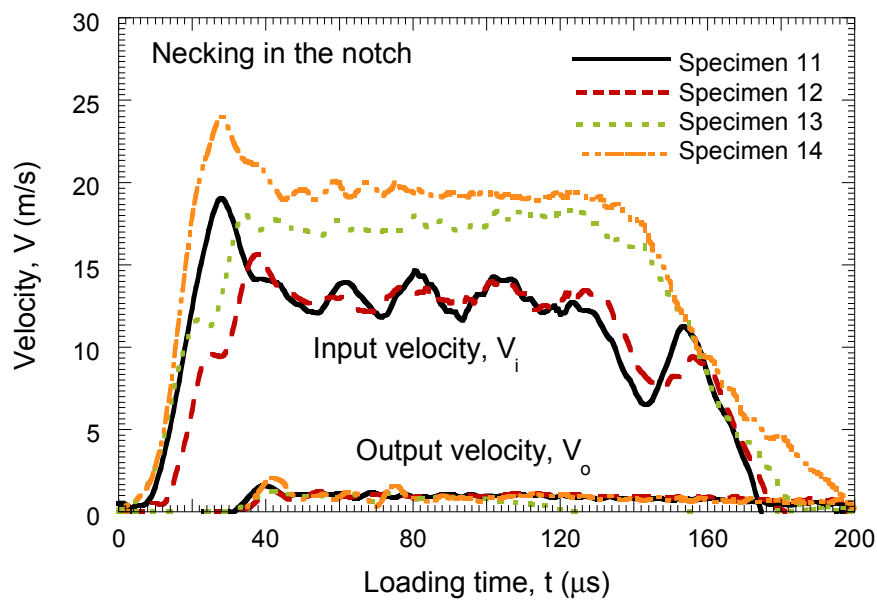
Table 4. Summary of the dynamic tensile tests carried out on centrally notched specimens.



(a)



(b)

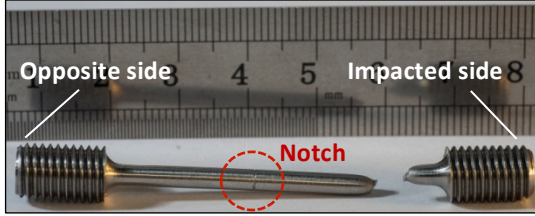


(c)

Fig. 5. Input and output velocity profiles of the dynamic tensile tests carried out on centrally notched specimens. (a) Tests for which the neck is located in the impacted side, (b) tests for which the neck is located in the opposite side, (c) tests for which the neck is located in the notch.

Necking in the impacted side

Specimen 6 – $V_0 \approx 15$ m/s

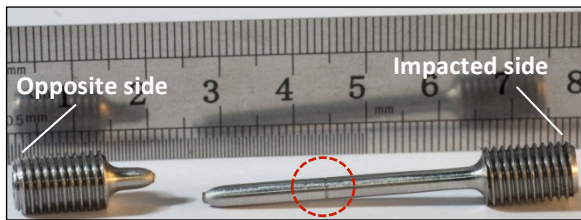


Specimen 7 – $V_0 \approx 15$ m/s

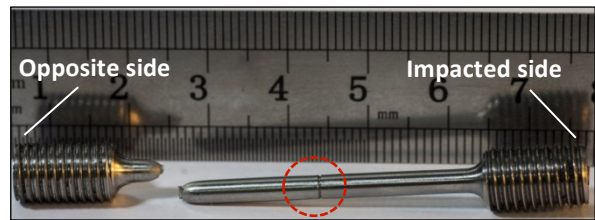


Necking in the opposite side

Specimen 8 – Peak velocity ≈ 25 m/s

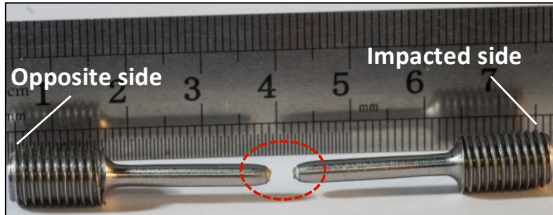


Specimen 10 – $V_0 \approx 18$ m/s



Necking in the notch

Specimen 12 – $V_0 \approx 13$ m/s



Specimen 13 – $V_0 \approx 17$ m/s

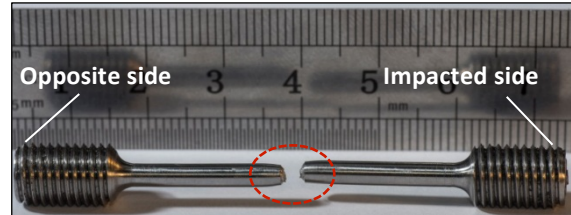


Fig. 6. Tested centrally notched specimens.

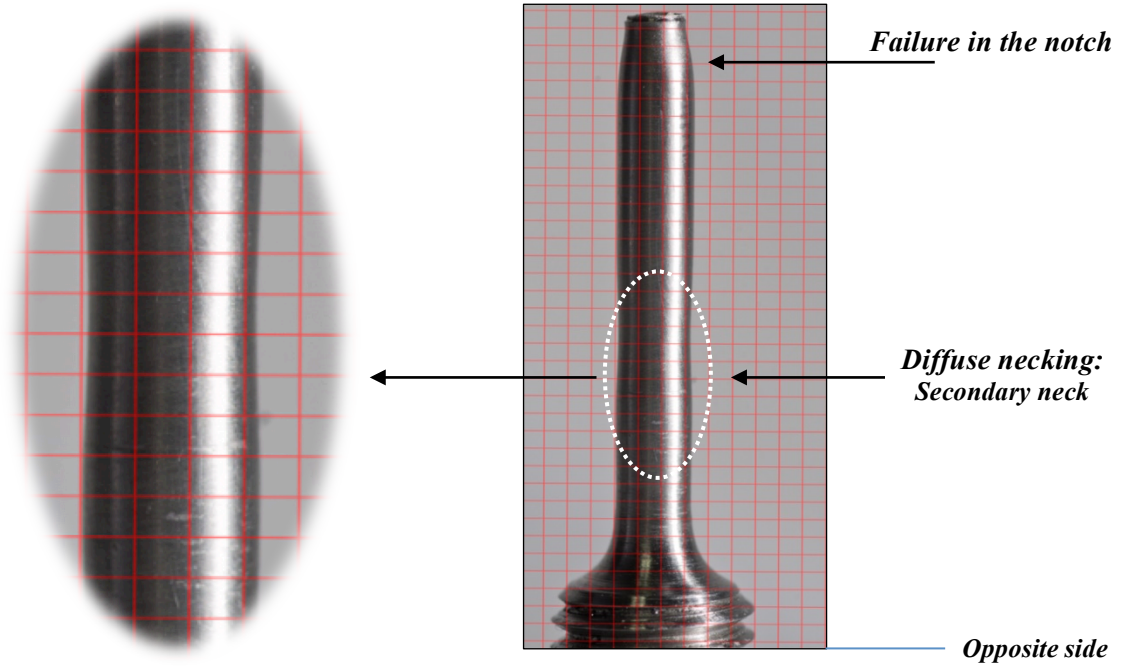


Fig. 7. Post mortem observation. Specimen 14. Fracture in the notch and secondary (diffuse) neck in the opposite side.

To gain further experimental insight into the notch-neck location interplay, we consider specimen 5 that was impacted at about 17 m/s and failed on the opposite side. Additional tests were carried out on same geometry specimens, similar applied velocity (~ 16 m/s), but this time, the notch was machined at $1/3$ of the gauge length (locations M and L in Fig. 1). A total of 4 experiments were carried out, namely 2 specimens with the notch at $1/3$ of the gauge length on the impacted side (location M) and the other 2 with the notch at $2/3$ of the gauge length, that is at $1/3$ of the gauge length on the transmitted side (location L), Table 5. The applied velocity profiles are shown in Fig. 8, showing that apart from the notch location, the boundary conditions were highly repeatable. As expected for this value of the input velocity (magnitude of the stress wave induced by the impact), necking and fracture take place close to the opposite side of the specimen. Consequently, when the notch was on that side, fracture occurred in the notch, but when it was placed on the incident side, necking still occurred close to the opposite side, therefore outside the notch. Those tests are quite instructive since they first of all strengthen the point that, for identical applied velocities, the results are quite repeatable and predictable. Moreover the results show once again that the presence of the notch in the specimen may or may not affect the location of the neck and subsequent fracture,

indicating that the presence of a weakest point in the structure will not necessarily dictate the failure locus at high loading rates, Fig. 9. It is assumed that this behavior is caused by the major role that inertia and stress waves play in the response of the material under impact loading.

Specimen	Input velocity, V_i (m/s)	Output velocity, V_o (m/s)	Notch location	Neck location
#15	15.0 (average)	1.0 (average)	<i>M</i>	<i>Opposite side</i>
#16	15.0 (average)	1.0 (average)	<i>L</i>	<i>Opposite side-Notch</i>
#17	15.0 (average)	1.0 (average)	<i>M</i>	<i>Opposite side</i>
#18	15.0 (average)	1.0 (average)	<i>L</i>	<i>Opposite side-Notch</i>

Table 5. Summary of the dynamic tensile tests carried out on sided notched specimens.

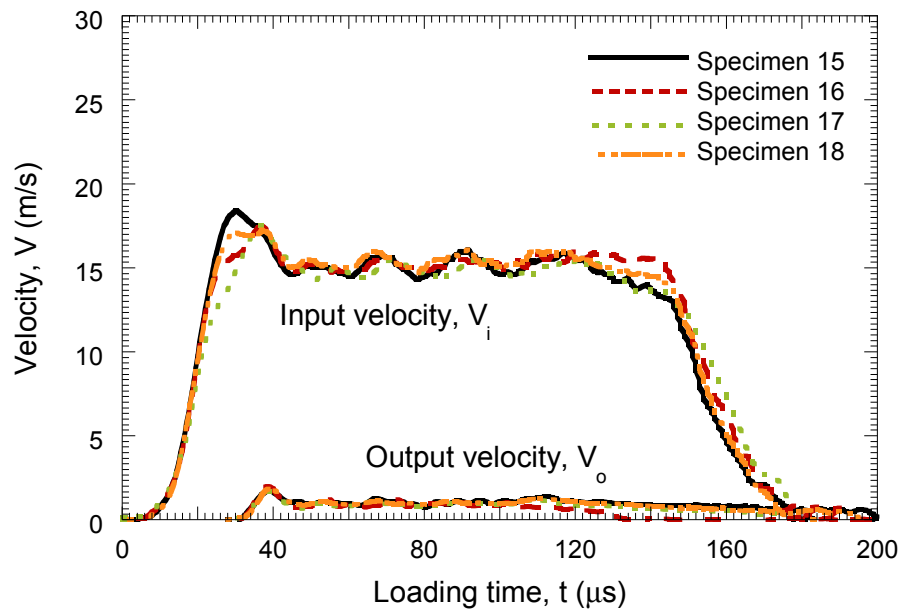


Fig. 8. Input and output velocity profiles of the dynamic tensile tests carried out on sided notched specimens.

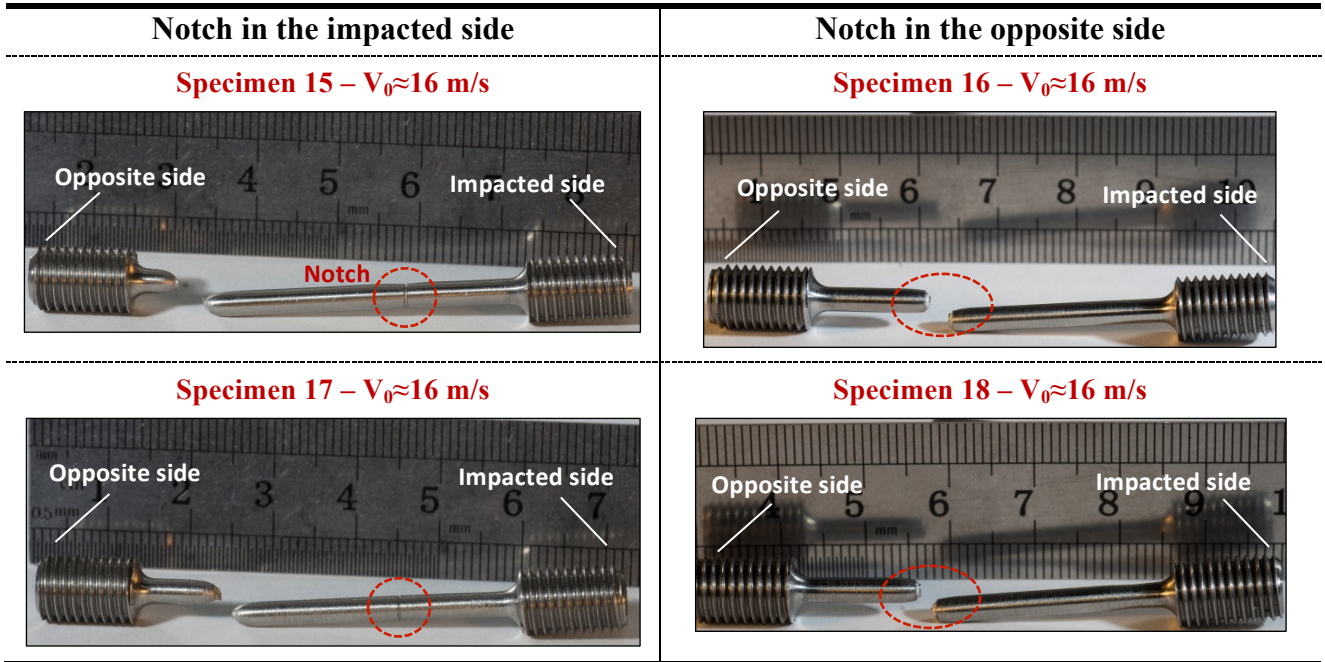


Fig. 9. Tested sided notched specimens.

One last point concerns the overall strain to fracture of the notched vs. smooth tested specimens, as it is important to assess whether the presence of a notch in the structure affects its energy absorption capacity. The appendix section presents the high speed recordings of the specimens' deformation until full neck formation (and fracture in some cases). Given the oscillations of the velocity measurements intrinsic to the dynamic character of the tests, one can calculate the macroscopic elongation of the specimen until inception of the neck. The recordings shown in the appendix show that the variability of the calculated macroscopic ductilities (sample deformation at the onset of the necking) is relatively small, which suggests that the presence of the notch in the specimen does not affect, to a first extent, the macroscopic ductility of the tested specimens. For all the tested specimens, with and without notches, the macroscopic strain to necking varies between 4 % and 5% (see Appendix section).

5. Discussion

This paper is of an experimental nature, aiming to assess the effects that a stress concentrator (notch) may have on a dynamically tensile tested structure. Before discussing further the main outcomes of this work, one should emphasize the context of the study with respect to the weakest link theory that was repeatedly invoked here. The weakest link theory was originally developed for brittle fracture in the quasi-static regime whereas the present work concerns dynamic failure of a ductile material. Hence, one of the goals of this work was to assess the extent to which the weakest link approach can be generalized to dynamic ductile failure. In the present context, one should also mention recent work about dynamic tensile loading of smooth specimens made of ductile steel (Osovski et al., 2013). In that study, emphasis was put on the deterministic (thus predictable) nature of the neck location, showing the latter could be reproduced by a numerical model provided care was taken to apply the prevailing boundary conditions. In a sense, the present work is a continuation of our previous work, with the emphasis placed this time on the influence of a geometrical discontinuity (notch) in the specimen.

First of all, one should note that the notches of this study cannot be considered as shallow defects. On the contrary, they are relatively short-wavelength, sharp and deep imperfections, whose depth reaches 0.1 of the specimen diameter.

Experiments of a similar nature have not been previously reported in the literature to the best authors' knowledge, perhaps because one natural assumption would be that failure always occurs in the stress concentrator, based on the quasi-static experience. However, the present results show that it is not necessarily so. Depending on the applied input velocity (magnitude of the stress wave induced by the impact), while the output velocities remain at a comparable level in all tests, one observes that the neck can locate on the impacted side at the lower tested velocity, ending on the

opposite side of the specimen for the higher tested velocities. Yet, some specimens fractured in the notch without apparent pattern in terms of velocity, a fact that seems to be related to some variability in the groove geometry. One should note that the reported trend in neck location is only partial, as the range of applied velocities did not exceed some 25 m/s while a full picture would be obtained had higher velocities been applied. Unfortunately, the current experimental setup did not allow for reaching much higher velocities. However, the reported results nevertheless indicate a clear trend in the variation of neck location with respect to the prescribed impact velocity (magnitude of the stress wave induced by the impact), and most of all that necking does not necessarily take place in the notch. In other words, the number of observed exceptions to the “anticipated rule” of notch induced necking is largely sufficient to question the latter assumption.

The results also show that, to a first extent, the macroscopic ductility of the dynamically tested specimens is not affected by the presence of a notch. In fact, while the quasi-static ductility (necking strain) of a notched specimen drops tremendously with respect to that of a smooth specimen (Fig. 1) our results show that this is not the case for the dynamic tests (Appendix). Here, the sample elongation of both smooth and notched specimens reaches values of 4-5%, which are definitely comparable (perhaps slightly higher) to the quasi-static necking strain values of smooth specimens. This result shows that, in addition to skipping it, the notch does not affect the structural ductility of the specimen.

Finally, while the results shown here are experimental, it is clear that future work should concentrate on capturing the observed effects in a numerical model that will allow optimized design of such impacted slender structures. This is work under progress.

6. Conclusions

Dynamic tensile testing of ductile steel specimens, with and without sharp notches, has been systematically carried out, keeping in mind the development of guidelines for the design of impacted structures. The main conclusions of this work can be summarized as follows:

- The location of the neck is deterministic and not random.
- The presence of sharp geometrical imperfections does not necessarily dictate the locus of the neck inception. The latter may skip the notch under suitable impact velocities.
- In the present investigation, one can observe that the dynamic ductility of the specimen (necking strain) is not reduced by the presence of the notch.
- Consequently, unlike the quasi-static case, a straightforward extension of the weakest point assumption to dynamically deforming ductile materials is contradicted by the present experimental observations.

Acknowledgements

D. Rittel acknowledges the support of Carlos III University with a Cátedra de Excelencia funded by Banco Santander during academic year 2011-2012.

The researchers of the University Carlos III of Madrid are indebted to the Ministerio de Ciencia e Innovación de España (Projects DPI/2011-24068 and DPI/2011-23191) for the financial support.

The authors thank Mr. A. Godinger for his technical support.

References

Altenhof W., Zamani N, North W., Arnold B. Dynamic stress concentrations for an axially loaded strut at discontinuities due to an elliptical hole or double circular notches. *Int J Impact Engng* 2004, 255-274.

Coker E. G. The Effects of Holes and Semi-Circular Notches on the Distribution of Stress in Tension Members, *Proc. Phys. Soc.* 1912-1913, p. 95.

Coker E. G., Chakko K. C., Satake Y. Photoelastic and strain measurements of the effects of circular holes on the distribution of stress in tension members, *Proc Instn of Engrs and Shipbuilders in Scotland*, 1919-1920, p. 34.

Gerlach R., Sathianathan S.K., Siviour C., Petrinic N. A novel method for pulse shaping of Split Hopkinson tensile bar signals. *Int J Impact Engng* 2011, 38, 976-980.

Howland R. C. J. On the Stresses in the Neighborhood of a Circular Hole in a Strip Under Tension, *Phil. Trans. Royal Soc. of London A* 229, 1929, p. 49.

- Inglis C. E. Stresses in a plate due to the presence of cracks and sharp corners, Spring meetings of the fifty-fourth session of the Institution of Naval Architects, 1913
- James W. G., North W. P. T. Dynamic stress concentration using the photoelastic technique. *J Strain Anal* 1969, 4, 261–6.
- Matsumoto H., Adachi T., Kakuham Y., Fukuzawa K. Analysis of the dynamic stress concentration factor by the two-dimensional boundary element method. *Int J Japan Soc Mech Eng, Series A* 1990, 33, 37–43.
- Nakayama N., Ohashi M., Takeishi H. Dynamic stress concentration in a strip plate with fillet. *Int J Japan Soc Mech Eng, Series A* 1998, 41, 326–31.
- Neuber H. Zur theorie der technischen formzahl, *Forschung im Ingenieurwesen* 1936, 7:6,271-274.
- Neuber H. Theory of notch stresses. Springer, Berlin. 1958.
- Osovski S., Rittel D., Rodríguez-Martínez J. A., Zaera R. Dynamic tensile necking: influence of specimen geometry and boundary conditions. *Mechanics of Materials*. Accepted for Publication.
- Preuss E. Forschungsarbeiten (Mitteilungen über Forschungsarbeiten), V.D.I., no. 126, 1912, and no. 134, 1913.
- Peterson R. E. Stress-Concentration Phenomena in Fatigue of Metals. A.S.M.E. Trans., 1933, APM-55-19.
- Peterson R. E. Stress Concentration Design Factors. John Wiley and Sons, New York, 1953.
- Rodríguez-Martínez J. A., Rusinek A., Arias A. Relation between strain hardening of steel and critical impact velocity in tension. *Journal of Theoretical and Applied Mechanics* 47 (2009) 645-665.

Rodríguez-Martínez J. A., Vadillo G., Zaera R., Fernández-Sáez J. On the complete extinction of selected imperfection wavelengths in dynamically expanded ductile rings. *Mechanics of Materials* 60 (2013) 107 – 120

Rusinek A., Zaera R., Klepaczko J. R., Cheriguene R. Analysis of inertia and scale effects on dynamic neck formation during tension of sheet steel. *Acta Materialia* 2005;53:5387-400.

Sørensen, N.J., Freund, L.B., 2000. Unstable neck formation in a ductile ring subjected to impulsive radial loading. *International Journal of Solids and Structures* 37, 2265-2283.

Strandberg M. Upper bounds for the notch intensity factor for some geometries and their use in general interpolation formulae. *Engineering Fracture Mechanics* 2001, 68, 577-585.

Zhang H., Ravi-Chandar K., On the dynamics of necking and fragmentation - I. Real-time and post-mortem observations in Al 6061-O. *Int J Fract* 2006, 142, 183–217.

Zhang H., Ravi-Chandar K., On the dynamics of necking and fragmentation - II. Effect of material properties, geometrical constraints and absolute size. *Int J Fract* 2008, 150, 3-36.

Zappalorto M., P. Lazzarin P. Strain energy-based evaluations of plastic notch stress intensity factors at pointed V-notches under tension, *Engineering Fracture Mechanics* 2011, 78, 2691–2706.

Specimen 2 – Smooth sample – Necking in the impacted side

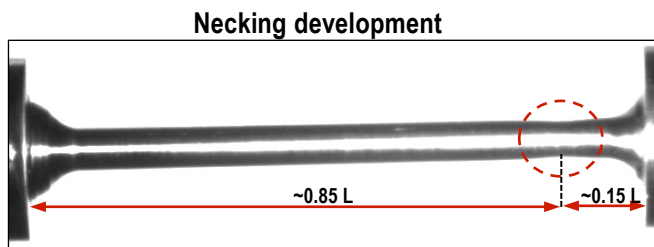
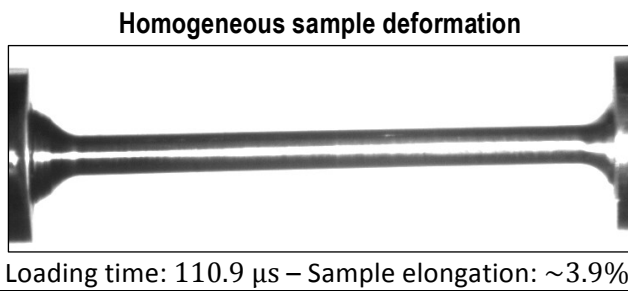



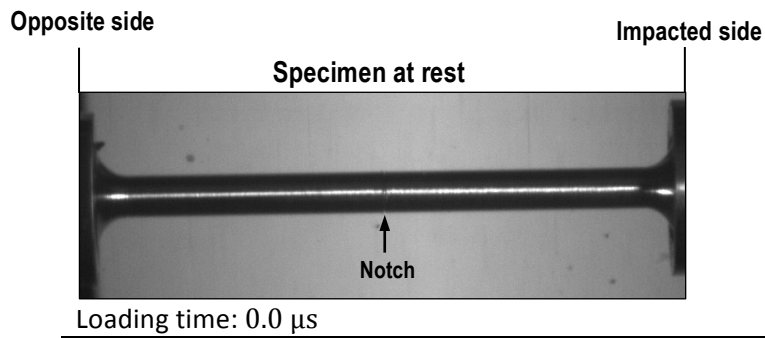
Fig. A1. Video sequence corresponding to specimen 2.

Impacted side

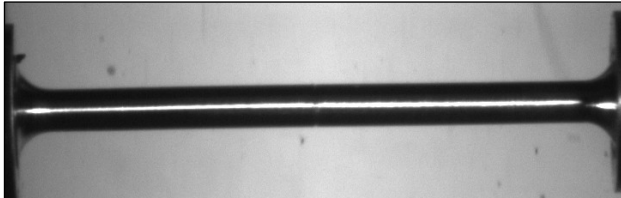
Specimen at rest

A photograph of a cylindrical specimen, likely a metal rod, lying horizontally. The specimen has a uniform diameter and is shown in its full length. The ends of the specimen are slightly flared or have a different texture, possibly indicating where it was attached to a testing machine. The background is a plain, light color.

Specimen 6 – Centrally notched sample – Necking in the impacted side

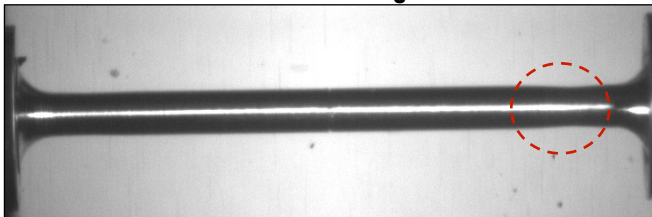


Homogeneous sample deformation



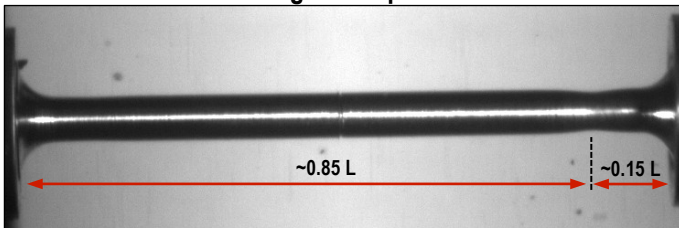
Loading time: 59.9 μs – Sample elongation: $\sim 2.0\%$

Onset of necking



Loading time: 118.96 μs – Sample elongation: $\sim 4.0\%$

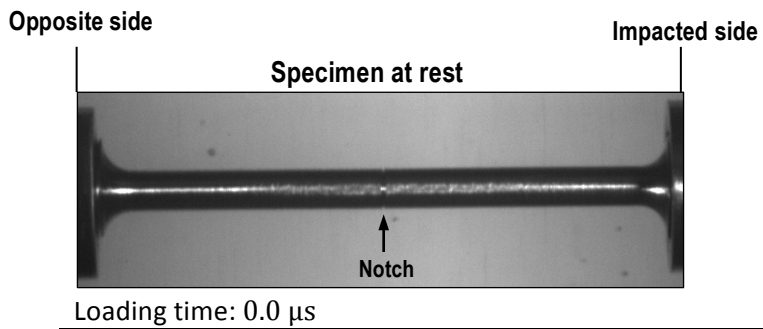
Necking development



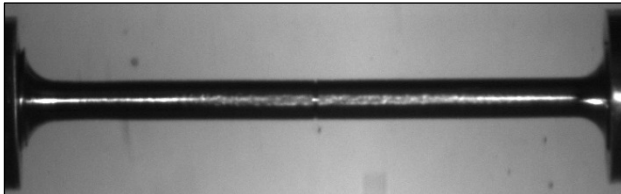
Loading time: 138.6 μs – Sample elongation: $\sim 4.7\%$

Fig. A3. Video sequence corresponding to specimen 6.

Specimen 9 – Centrally notched sample – Necking in the opposite side

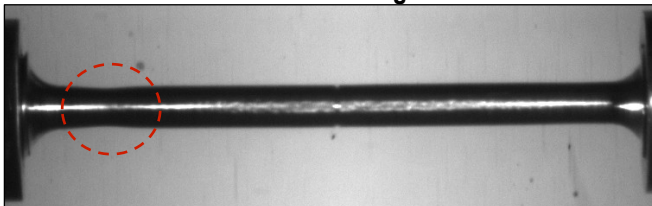


Homogeneous sample deformation



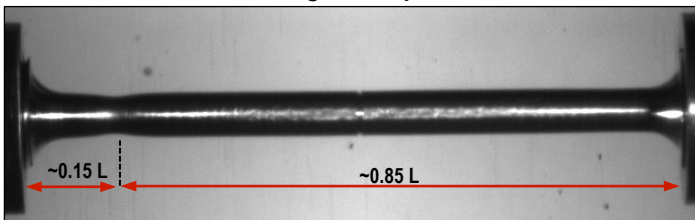
Loading time: 79.3 μs – Sample elongation: $\sim 1.9\%$

Onset of necking



Loading time: 138.1 μs – Sample elongation: $\sim 3.3\%$

Necking development



Loading time: 197.0 μs – Sample elongation: $\sim 4.7\%$

Fig. A4. Video sequence corresponding to specimen 9.

Specimen 13 – Centrally notched sample – Necking in the notch

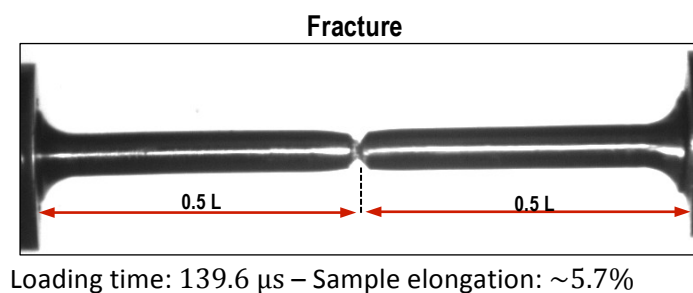
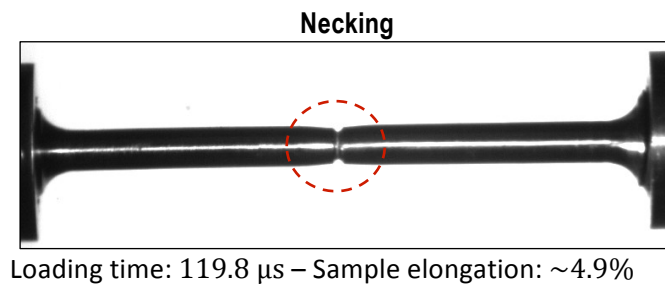
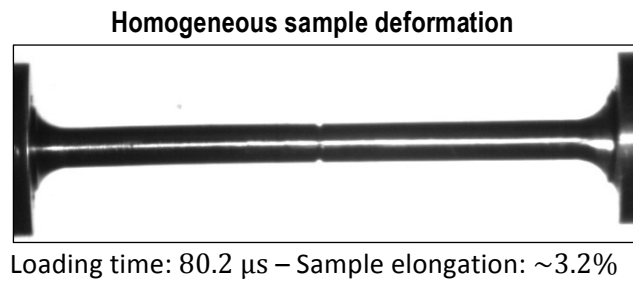
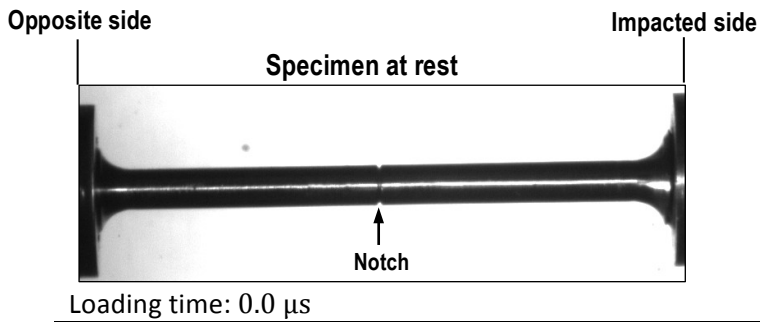
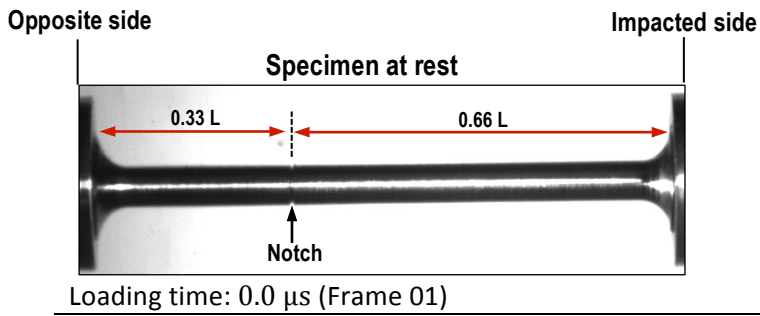
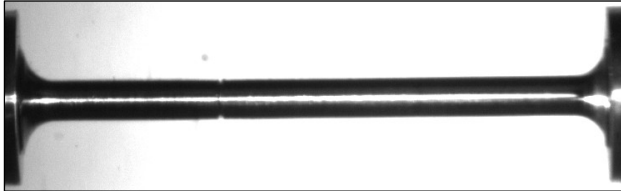


Fig. A5. Video sequence corresponding to specimen 13.

Specimen 16 – Sided notched sample – Necking in the opposite side/notch

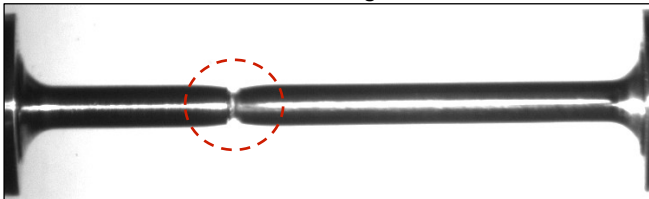


Homogeneous sample deformation



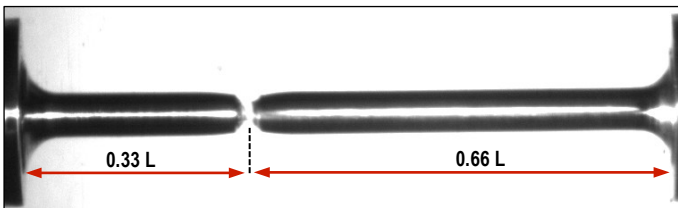
Loading time: 98.2 μ s – Sample elongation: $\sim 3.3\%$

Necking



Loading time: 155.0 μ s – Sample elongation: $\sim 5.2\%$

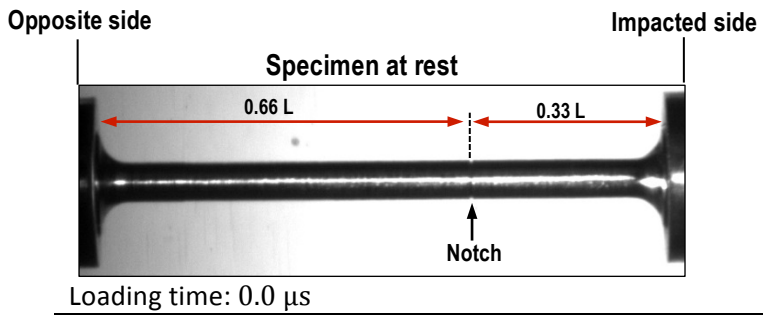
Fracture



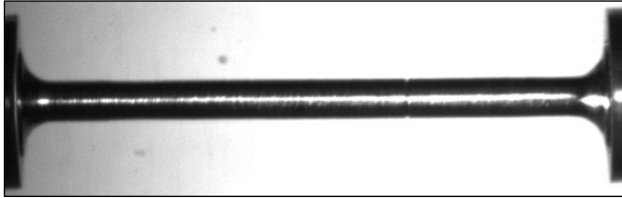
Loading time: 184.0 μ s

Fig. A6. Video sequence corresponding to specimen 16.

Specimen 17 – Sided notched sample – Necking in the opposite side

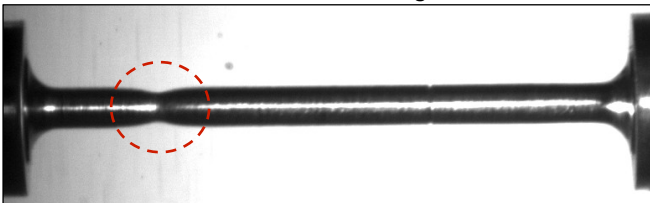


Homogeneous sample deformation



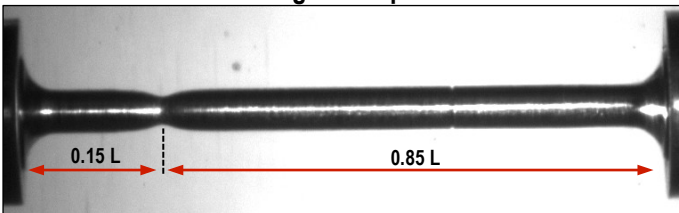
Loading time: 62.3 μ s – Sample elongation: \sim 2.1%

Onset of necking



Loading time: 137.2 μ s – Sample elongation: \sim 4.7%

Necking development



Loading time: 162.3 μ s – Sample elongation: \sim 5.5%

Fig. A7. Video sequence corresponding to specimen 17.